

**Fe₇Se₈ Encapsulated in N-doped Carbon Nanofibers as Stable Anode Materials
for Sodium Ion Batteries**

Le Hu^{1#}, Chaoqun Shang^{1#*}, Xin Wang^{1,2,3*}, Guofu Zhou^{1,2,3}

¹ Guangdong Provincial Key Laboratory of Optical Information Materials and Technology & Institute of Electronic Paper Displays, South China Academy of Advanced Optoelectronics, South China Normal University, Guangzhou 510006, China

² National Center for International Research on Green Optoelectronics, South China Academy of Advanced Optoelectronics, South China Normal University, Guangzhou 510006, China

³ International Academy of Optoelectronics at Zhaoqing, South China Normal University, Zhaoqing 526000, China

#These authors contributed equally.

*Corresponding author:

chaoqun.shang@ecs-scnu.org

wangxin@scnu.edu.cn

Material Characterization

The morphology of all the samples was observed by a field emission scanning electron microscope (FESEM, Zeiss Ultra 55) and a transmission electron microscope (TEM, JEOL JEM-2100F). Thermal gravimetric analysis (TGA, SDT Q600 TG-DTA) was carried out to confirm the content of Fe₇Se₈. The crystal phase was investigated by x-ray diffraction (XRD, Bruker D8 advance). The surface chemical compositions were measured on an x-ray photoelectron spectrometer (XPS, Kratos AXIS Ultra DLD).

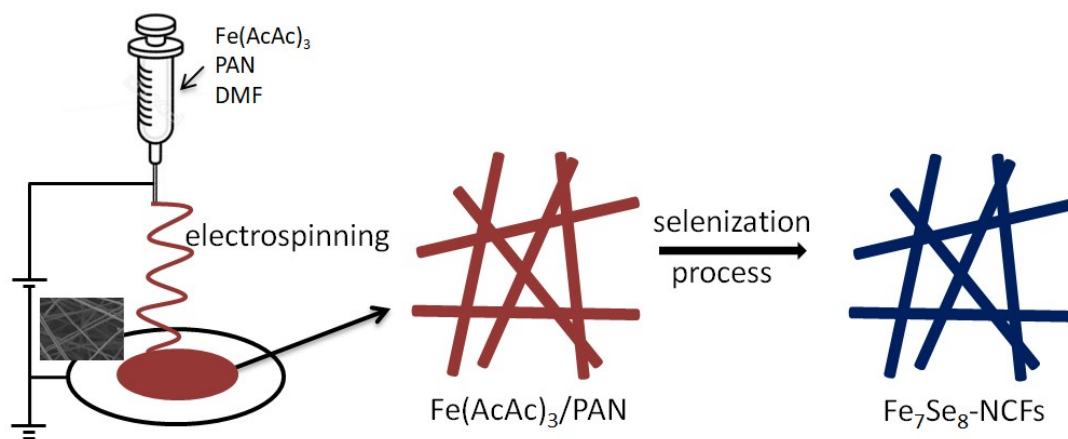


Figure S1. The schematic synthesis process of Fe_7Se_8 -NCFs nanofibers.

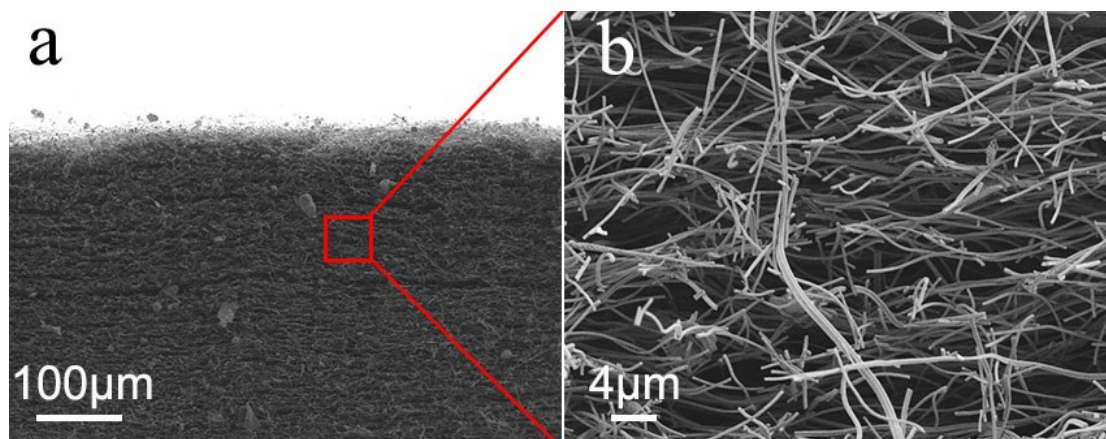


Figure S2. Cross-section SEM images of Fe_7Se_8 -NCFs nanofibers.

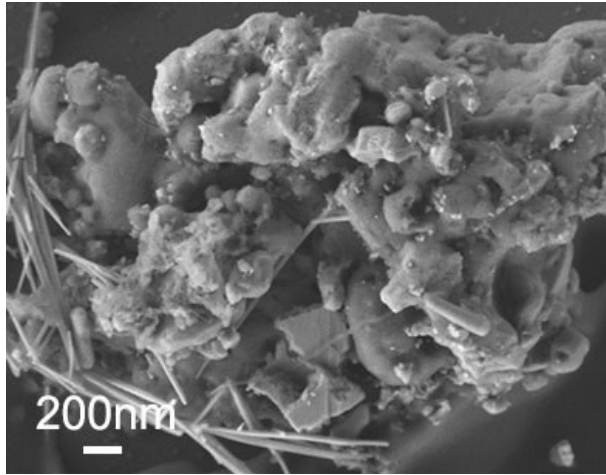


Figure S3. SEM image of bulk Fe₇Se₈.

The crystal size is calculated by the Scherrer's equation as follows:

$$D = \frac{K\lambda}{\beta \cos\theta}$$

Here, D is the average crystal diameter, K is a constant related the shape of the crystallites, λ is the wavelength of the X-rays employed, β is the corrected peak width (full width at half-maximum) and θ is the diffraction angle.

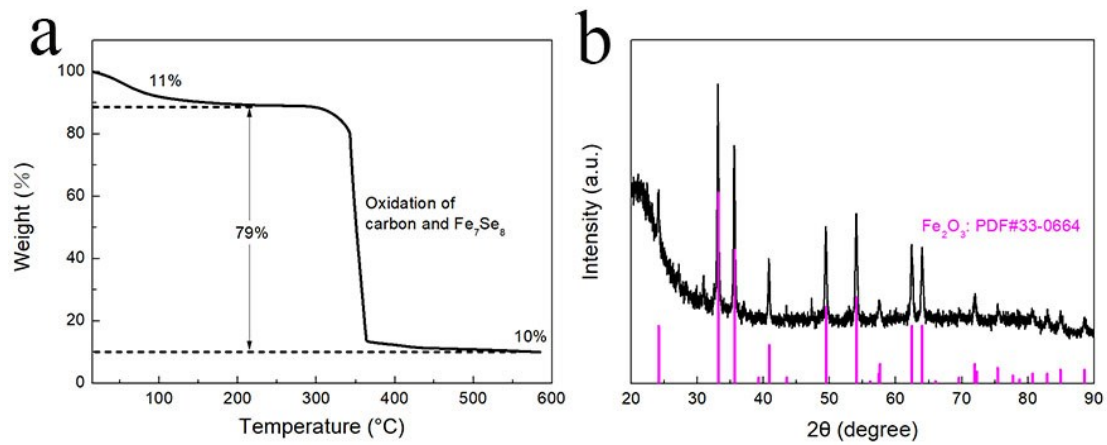
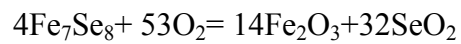


Figure S4. (a) the TGA spectra of Fe₇Se₈-NCFs; (b) the combustion product of Fe₇Se₈-NCFs.

The calculation of Fe₇Se₈ content in Fe₇Se₈-NCFs:



$$\text{Fe}_7\text{Se}_8 (\text{wt}\%) = \frac{4 \times \text{molecular weight of Fe}_7\text{Se}_8}{14 \times \text{molecular weight of Fe}_2\text{O}_3} \times \frac{\text{weight of Fe}_2\text{O}_3}{\text{weight of Fe}_7\text{Se}_8 - \text{NC}} \times 100\%$$

$$= \frac{4 \times 1022.6}{14 \times 159.7} \times \frac{1 - 0.79 - 0.11}{1 - 0.11} \times 100\%$$

$$= 20.6\%$$

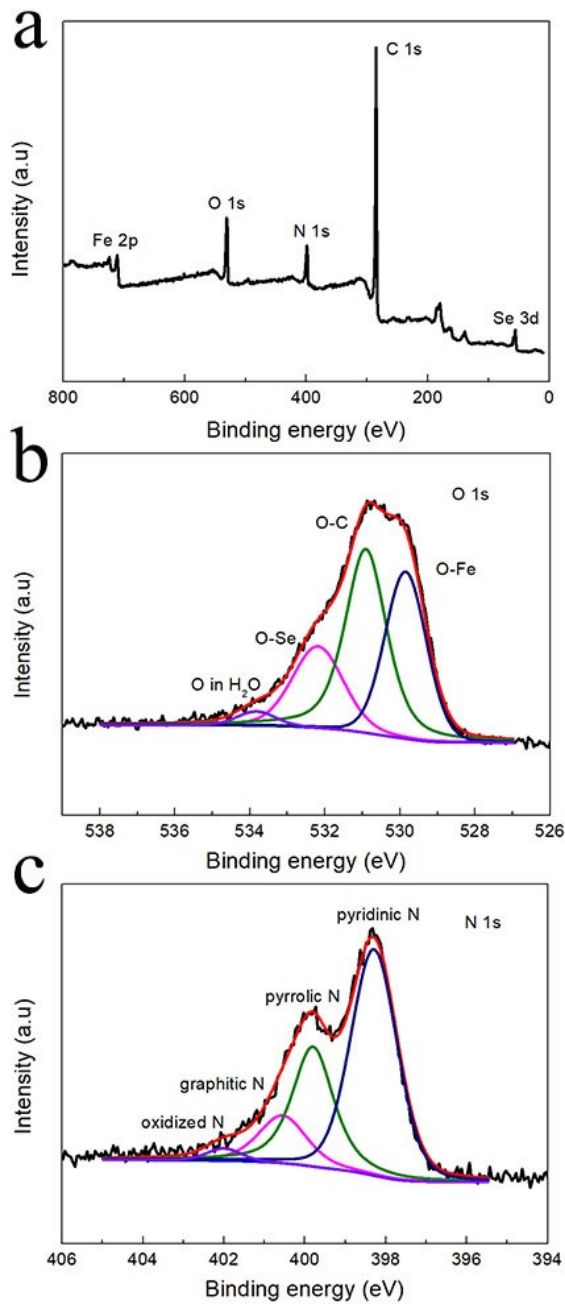


Figure S5. XPS survey spectra and corresponding (b) O 1s and (c) N 1s and (d) C 1s of the Fe₇Se₈-NCFs, respectively.

The O 1s spectrum is convoluted into four peaks at 533.8, 532.2, 530.9 and 529.8 eV, which are attributed to adsorbed water on the surface of sample, Se-O, C-O and Fe-O bonds (Figure S5b)[1]. The N 1s spectrum is deconvoluted into representative peaks centered at 402, 400.5, 399.8 and 398.3 eV, attributing to oxidized-N, graphitic-N, pyrrolic-N and pyridinic-N (Figure S5c)[2]

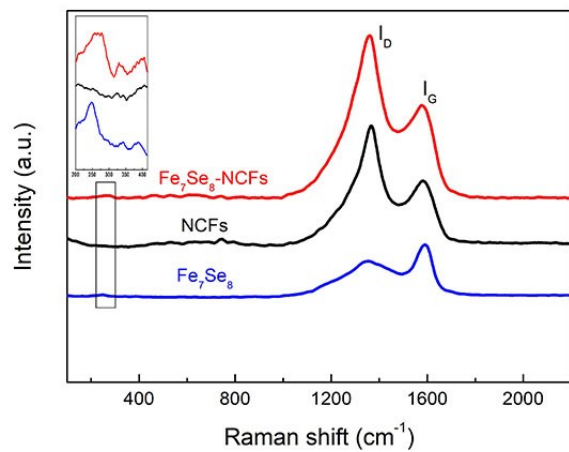


Figure S6. Raman spectra of Fe₇Se₈-NCFs, Fe₇Se₈ and NCFs, respectively.

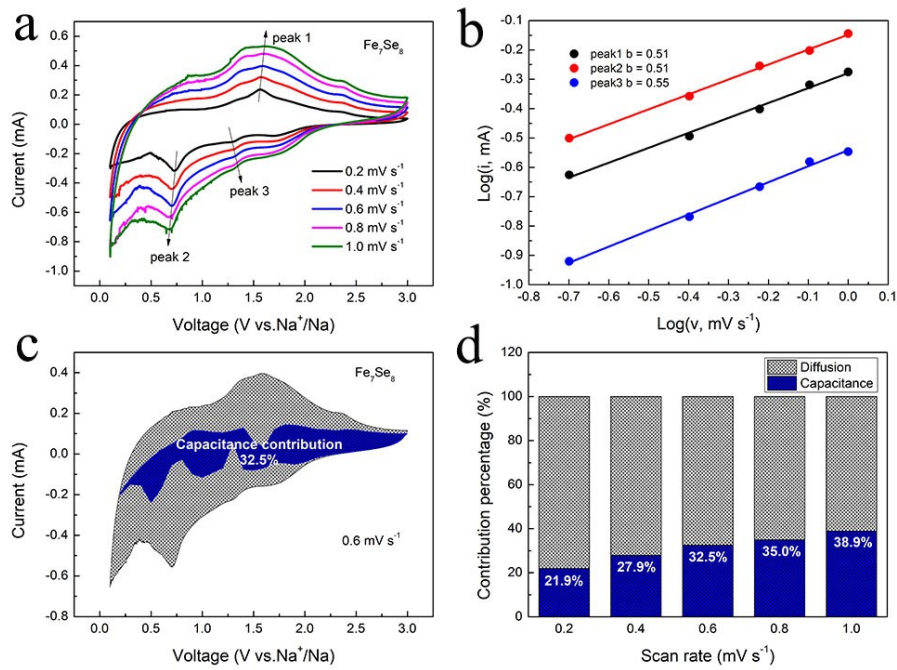


Figure S7. Kinetic analysis for sodium storage: (a) CV curves of Fe_7Se_8 at different scan rates; (b) fitting line of $\log(i)$ versus $\log(v)$ plots of MnSe; (c) capacitive and diffusion-controlled contribution of Fe_7Se_8 at 0.6 mV s^{-1} ; (d) ratio of contribution capacitive of Fe_7Se_8 at different scan rates.

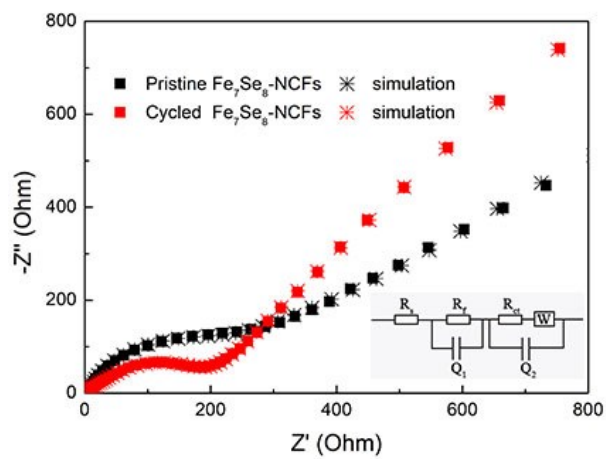


Figure S8. EIS curves at pristine and cycled state of Fe₇Se₈-NCFs.

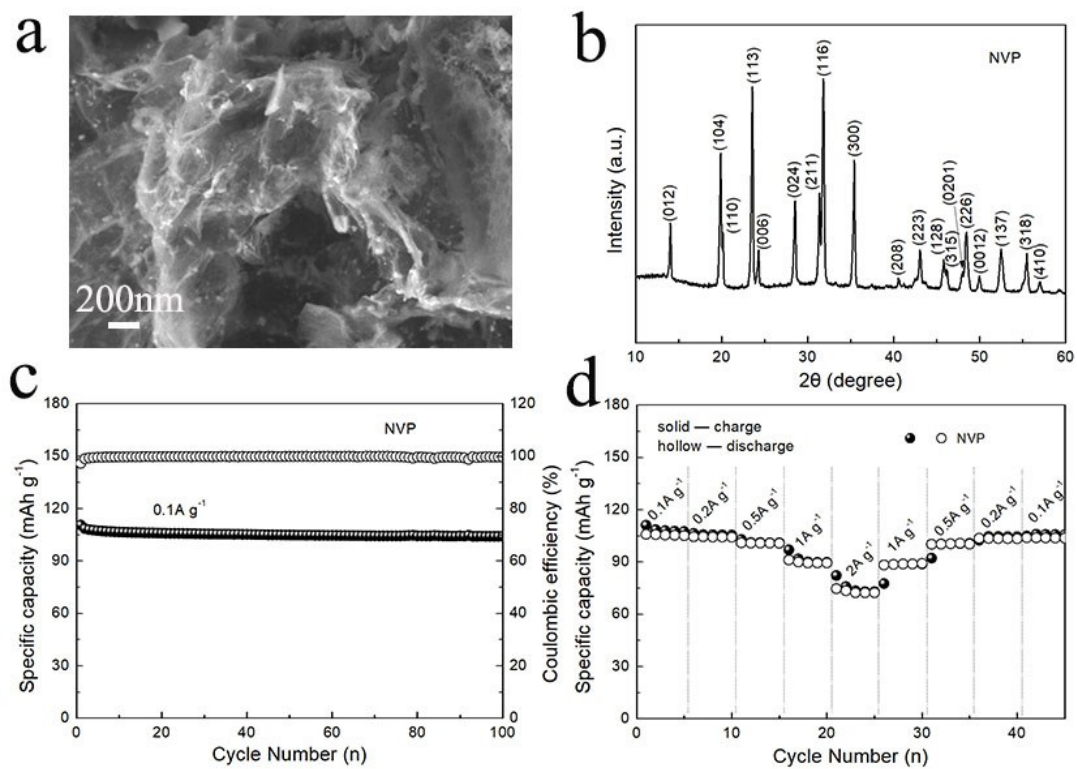


Figure S9. (a) SEM image and (b) XRD pattern of the NVP. (c) Cycling performance and (d) rate capability of the NVP cathode between 2.5 and 4.0 V in half cell.

Table S1. The comparison of electrochemical performance for Fe₇Se₈-NCFs and other Fe₇Se₈-based electrodes in sodium storage.

Samples	Sodium ion batteries	
	Cycling performance (reversible capacity)	Rate performance
Fe ₇ Se ₈ -NCFs (This work)	148 mAh g ⁻¹ at 2 A g ⁻¹ (2000 cycles)	153 mAh g ⁻¹ at 2 A g ⁻¹
Fe ₇ Se ₈ /N-CNF (Ref. 12)	405.6 mAh g ⁻¹ at 0.1 A g ⁻¹ (500 cycles)	364 mAh g ⁻¹ at 2 A g ⁻¹
Fe ₇ Se ₈ @C/N NBs (Ref. 14)	385 mAh g ⁻¹ at 0.1 A g ⁻¹ (350 cycles)	320 mAh g ⁻¹ at 2 A g ⁻¹
Fe ₇ Se ₈ @C (Ref. 21)	399 mAh g ⁻¹ at 0.5 A g ⁻¹ (150 cycles)	353 mAh g ⁻¹ at 2 A g ⁻¹
Fe ₇ Se ₈ @NC (Ref. 25)	367 mAh g ⁻¹ at 0.5 A g ⁻¹ (400 cycles)	251 mAh g ⁻¹ at 2 A g ⁻¹
Fe ₇ Se ₈ NRBs (Ref. 29)	300 mAh g ⁻¹ at 0.5 A g ⁻¹ (500 cycles)	245 mAh g ⁻¹ at 2 A g ⁻¹

Reference:

- [1] C. Yuan, J. Li, L. Hou, X. Zhang, L. Shen, X.W.D. Lou, Ultrathin Mesoporous NiCo₂O₄ Nanosheets Supported on Ni Foam as Advanced Electrodes for Supercapacitors, *Adv. Funct. Mater.*, 22 (2012) 4592-4597.
- [2] Q. Zhao, R. Bi, J. Cui, X. Yang, L. Zhang, TiO_{2-x} Nanocages Anchored in N-Doped Carbon Fiber Films as a Flexible Anode for High-Energy Sodium-Ion Batteries, *ACS Appl. Energy Mater.*, 1 (2018) 4459-4466.